Research on Trajectory and Modeling of Body Movement

Biyuan Yao[1], Jianhua Yin[2], Guiqing Li[1], Hui Zhou[3], Lixin Liu[4]

[1] School of Computer Sci. and Eng., South China University of Technology, China
[2] School of Sci., Hainan University, China
[3] School of Computer Sci. and Cyberspace Security, Hainan University, China
[4] Institute of Deep-sea Sci. and Eng., Chinese Academy of Sciences, China
yaobiyuanyy@163.com, yinjh@hainu.edu.cn, ligq@scut.edu.cn, zhouhui@hainu.edu.cn, liulx@idsse.ac.cn

Abstract

Body movement analysis and identification are challenging due to high-dimension data, and can be disturbed by moving speed and position of a certain person. This paper is aiming to establish a limb trajectory model to reveal the hidden information of limb activities. According to the data onto nine parts of the human body, a three-dimension view of body activities is proposed to analyze limb positions in continuing status, represented by a sequence of body movement of the data in a three-dimension space coordinate. The motion equations of the body are obtained by regression functions under normal state and active state. The experiment of ten definitions of action shows that head, elbows, wrists, knees and ankles are strongly connected when an activity is performed.

Keywords: Movement identification, 3-Dimension trajectory, Regression analysis

1 Introduction

Movement trajectory refers to the spatial characteristics of the movement of a part of the body from the beginning to the end. The motion trajectory is represented by the direction of motion trajectory, the form of motion trajectory and the amplitude of motion. The movement of the human body is in the process of head, human limbs, trunk posture and movement. It is an interaction between people and the outside world, also shows a certain intention or purpose of human [1]. Pattern recognition is the method of processing and analyzing various forms of information representing things or phenomena, so as to describe, identify, classify and interpret things or phenomena. It is an important aspect of information science and artificial intelligence [2]. The recognition of human action refers to the process of automatic detection, analysis and understanding all kinds of human activities and behaviors in order to judge people's intentions and provide corresponding services [3]. The contemporary movement recognition algorithms cannot accurately locate all the parts of the body. Because of the current body recognition algorithm, it is impossible to accurately locate all parts of the body. Therefore, the core of this research is to use the correct information on limb movements extracted to design an effective feature of a high discriminant force, and to identify the movements of the limbs according to this feature.

The study of three-dimensional human movement towards capture technology is to acquire accurately the three-dimensional human body's movement in all kinds of sensor technology. The essence of recognition in human motion is a pattern classification problem. So we study it from feature extraction and classification matching. Through the analysis of human movement, it can be found that the movements of the human body can be broken down into various parts of body movement, such as head movement, hand movement, foot movement and so on. The data used for recognition in human motion are acquired mainly by the VICON of three-dimensional gait analysis system. The data selected ten people in normal and active state of body movements as test samples, including seven men and three women. The data acquisition process is placed on the head, left arm (elbow and wrist), right arm (elbow and wrist), left leg (knee and ankle) and right leg (knee and ankle) for 3D data acquisition markers. By changing the mutual displacement between different joints and the state of motion, you can achieve the desired effect of limb movement. The body movement of each tester corresponds to a time series of approximately 3000 samples with a sampling frequency of 200Hz. The database has 540 movement sequences, including 20 major categories, and there are 9 similar but different movements in each category. Because of the differences in the nine parts of the human body, the number of key parts collected by the VICON motion capture system is also different. Because the experiment select 10 people to carry out different body movements towards different displacement, the corresponding information on the test site is reserved for each subject only once. The first three features are the features of the first segment, features 4, 5 and 6 are features of the second type of the segment, and so on. Finally, the whole sequence of

*Corresponding Author: Jianhua Yin; E-mail: yinjh@hainu.edu.cn
DOI: 10.3966/160792642019102006020

motion is formed, which is shown in Table 1.

Table 1. Characteristics of the whole motion sequence

Segment	| Head | L-Arm | R-Arm | L-Leg | R-Leg |
Maker	| *m*1| *m*2 | *m*3 | *m*4 | *m*5 | *m*6 | *m*7 | *m*8 | *m*9 |
Coords	| *x y z* | *x y z* | *x y z* | *x y z* | *x y z* | *x y z* | *x y z* | *x y z* | *x y z* |
Column	| 1, 2, 3 | 4, 5, 6 | 7, 8, 9 | 10, 11, 12 | 13, 14, 15 | 16, 17, 18 | 19, 20, 21 | 22, 23, 24 | 25, 26, 27 |
Segment	[Head, Left arm (L-Arm), Right arm (R-Arm), Left leg (L-Leg), Right arm (R-Leg)]
Maker	[Arm markers: wrist (WRS), elbow (ELB), Leg markers: ankle (ANK), knee (KNE)]
Coords	The 3 coordinates (x,y,z) define the 3D position of each marker in space.

Note. http://archive.ics.uci.edu/ml/datasets/Vicon+Physical+Action+Data+Set.

2 Related Works

Human body gesture recognition is a hot research topic in the field of computer vision. It has a wide range of applications in the field of intelligent visual surveillance, video retrieval, human interaction and other fields, and more and more researchers are also concerned about it. In China, Xue Yang etc. from South China University of Technology uses the mobile phone of acceleration sensors to collect 10 kinds of movements in three positions of belts, pants and shirt pocket, and identify them by using three-dimensional trajectories and statistical methods. At the same time, a single accelerometer is used to complete the high jump height estimation [4]. Huang Qihua, Xiangtan University and other people use a gyroscope sensor to collect anthropological gesture information and transmit data to the PC through wireless communication. The support vector model is used to identify gesture actions with a recognition rate of up to 99.4% [5]. Lau and Tong use accelerometers and gyroscopes to monitor gait characteristics and identify walking status [6]. In foreign countries, Lyons and other people in Ireland use the dual-axis gyroscope to collect human data, using threshold settings and statistical methods to identify the tumbling movement of the human body [7]. Amft and others in the United States use four acceleration sensors to collect the arm movements of the subjects, through the identification algorithm to complete the recognition of the daily behavior of the subjects, such as eating and drinking, and then evaluate the health level of the individual's habits and habits [8]. Pansiot and others in the United Kingdom use inertial sensor systems to detect the movements of body swimming, which is used to assess the status of swimming [9]. Arvind and Valtazanos at the University of Edinburgh in the United Kingdom use accelerometers and gyroscopes to monitor the performance of double-dances and establish a physical model of the limbs of the two dancers [10]. It can be seen that many scholars have done a lot of research work, and have achieved more research results, which have greatly promoted the development of the research of human body movement and brought benefits for human society.

Motion captures technology is used to track the movement towards some or all of the human and animal joints through video cameras, motion sensors or other system devices. Motion information about the joints is measured to provide reference data onto gait analysis and video production [11]. At this stage, people capture the data of human movement through sensors, and then give these data to the virtual model, so that the virtual model has the same lifelike action as human beings [12-14]. Body movement detection research is ranging from video analysis to image processing, even extended to posture-graphic data model for movement classification [15]. Furthermore, action decomposition and function optimization of postures are designed for physical mechanism analyzing [16]. Yashiro et al. tried to determine the effect of inaccuracies in body segment parameters and modeling assumptions on the estimate of antero-posterior center of mass (COM) trajectory in [17]. These results provide helpful data in the processing method and physical mechanisms of basis for study of body movement. However, identifying correlations between couples of actions and identifying an unknown movement of data are still a challenge confronted with us [18-21].

3 Theoretical Basis

3.1 Descriptions of Body Movement

We take the body as a particle and regard it as an object of mass and space position, ignoring the size and shape of the body.

(1) Position vector is the vector from the origin of the coordinate of the position of the particle. Figure 1 is a rectangular coordinate system, and the position coordinates are the position vectors of xyz as the particle.

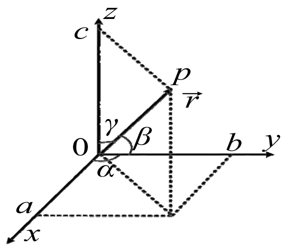

Figure 1. The position vector

The direction of r can be determined by directional cosine:

$$\vec{r}=a\vec{i}+b\vec{j}+c\vec{k}, \quad r=\left(a^{2}+b^{2}+c^{2}\right). \tag{1}$$

$$\cos\alpha=\frac{a}{r},\cos\beta=\frac{b}{r},\cos\gamma=\frac{c}{r} \tag{2}$$

(2) Equation of motion is the function of the position coordinates of particles and time. Among them, the vector type and scalar type are respectively as follows.

$$\vec{r}=a(t)\vec{i}+b(t)\vec{j}+c(t)\vec{k} \tag{3}$$

$$a=a(t),b=b(t),c=c(t) \tag{4}$$

(3) Trajectory equation. The equation (4) cancels out t, so that the relationship between a, b and c is the trajectory equation, that is, F (a, b, c) = 0.

3.2 Data Preprocessing

Distributed measure is a method of measuring measures by dividing the data sets into smaller subsets, calculating each of its own measures, and then combining the results of the calculations to obtain the metrics for the entire data set. The overall measure is a measure that must be calculated over the entire data. Calculation formula for standard deviation is as follows.

$$\hat{\sigma}=\sqrt{1/\left[(n-1)\sum_{i=1}^{n}\left(x_{i}-\bar{x}\right)^{2}\right]} \tag{5}$$

Qualitative prediction method mainly relies on some investigators, according to their own research experience to determine the general trend of physical movement in the future. Quantitative forecasting method is a method to analyze the future development trend of limb movement by using mathematical statistical method, econometric analysis of method and mathematical modeling. It is mainly through the analysis of historical statistics and bodies' movements. The development trend of human health is predicted by quantitative indicators. Quantitative prediction is mainly used to analyze and explain the development trend, increase and decrease of limb movement and the possible level of arrival. The process of identification with body movement is shown in Figure 2.

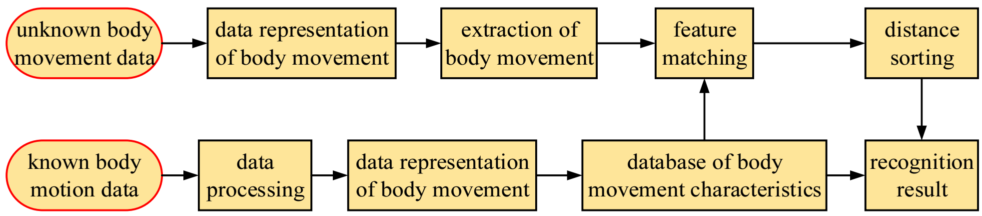

Figure 2. Body movement recognition

The task of feature extraction is to determine the data which is meaningful to the classification according to the measured data as the characteristic data. The purpose is to compose the features of recognition and classification through feature selection and extraction. Under the premise of guaranteeing the accuracy of a certain classification, we keep the classified information as much as possible and reduce the feature dimension, so that the classifier's work is fast and accurate. Feature extraction refers to making a set of metric values(x_1, x_2, …, x_L) generating some new m features (y_1, y_2, …, y_m) through some transformation as the feature of dimension reduction. Among them, i=1, 2, …, m, $m \le L$.

3.3 Matching Model

Let G is a graph, $M \subseteq E(G)$, for $\forall\, e_i, e_j \in M$, e_i and e_j aren't adjacent, then M is a matching of G. Matching two consecutive actions are the most critical step in action recognition. The process of matching action is actually to calculate the similarity between the input action and the action template for the database, and then think that the input action and the highest similarity action template is a kind. For the extracted features, the matching algorithm is used to analyze the correlation experiments and the experimental results, which shows the effectiveness of the algorithm in recognition of body movement.

3.4 Locations of Distance Difference

Since the collected data are constant, there is no velocity component. Therefore, a large number of repeated observations are carried out to improve the positioning accuracy. In $|A_mA_n|$, A_m and A_n represent the two-dimensional joint points of the human body parts, m and n respectively indicate the starting and ending index number of junction node, among them, $m<n$. Point (x_i, y_i, z_i) represents the spatial coordinate of the corresponding to the relevant nodes in the human body part, i($m \le i \le n$-1) represent the index variable of the

corresponding to the relevant nodes in the calculation, then the spatial fixed distance from the formula is

$$|A_m A_n| = \sum_{j=m}^{n-1} \sqrt{(x_j - x_{j+1})^2 + (y_j - y_{j+1})^2 + (z_j - z_{j+1})^2} \quad \textbf{(6)}$$

4 Model Simulation

4.1 Three-dimensional View of the Analysis

Depending on the position data given to the body, Figure 3 depicts the trajectory of the body movements, and then reflects the movement characteristics of the human body. It specifies the direction of the movement towards the three planes of the body's sagittal plane, the frontal surface and the vertical plane, as well as the six directions of the upper and the lower, the right and the left, the front and the rear.

The trajectories in Figure 3 show that the head, elbows, wrists, knees and ankles of the experimenter have a large amplitude movement, and the range of limb movement is a large and the frequency is fast. Figure 3(a) shows the movement of the elbow joint and the left arm at the elbow with a slight fluctuation in the curve, showing a curvilinear movement. The range of its horizontal position fluctuates between 520 and 1200 millimeters, and the fluctuation range of the vertical coordinate position is between -150 and 450 millimeters.

Figure 3(b) shows frontkick and right leg knee fluctuates with large fluctuations. Its horizontal position fluctuates in the range of 1000~1200 millimeters and 1280~1350 millimeters, and its position in the vertical coordinate range is -1100~-300 millimeters. Figure 3(c) shows the span of the hammer and the wrist of the right arm have the large span. It indicates that the motion of limbs is disorder, and the wave motion is large. The position of its coordinates is in the range of 400~1200mm, and the vertical position fluctuation range is -700~0mm. Figure 3(d) shows the header and head to fluctuate greatly. Its horizontal position fluctuates in range of 70~910 millimeters, and the vertical position fluctuation range is -900~-150 millimeters. Figure 3(e) shows the knee and left leg knee has the larger span. It indicates that the motion of limbs is disorder, and the wave motion is large. Figure 3(f) shows the pull and the wrist of the left arm fluctuates greatly. Figure 3(g) shows the span of punch and the elbow of the right arm is relatively concentrated. The volatility is not big. Figure 3(h) shows the span of the push and the elbow of the right arm is relatively concentrated, showing a diagonal movement. Figure 3(i) shows the span of the sidekick and left leg ankle is relatively concentrated, showing the motion of a projectile. Figure 3(j) shows the span of slap and right arm wrist has the larger span and fluctuates with large fluctuations. Figure 3(j) shows a downward trend and Figure 3(i) shows an upward trend. Figure 3 shows that elbows, punches, sidekicks, pushes and slaps do not have a significant displacement change in the course of movement.

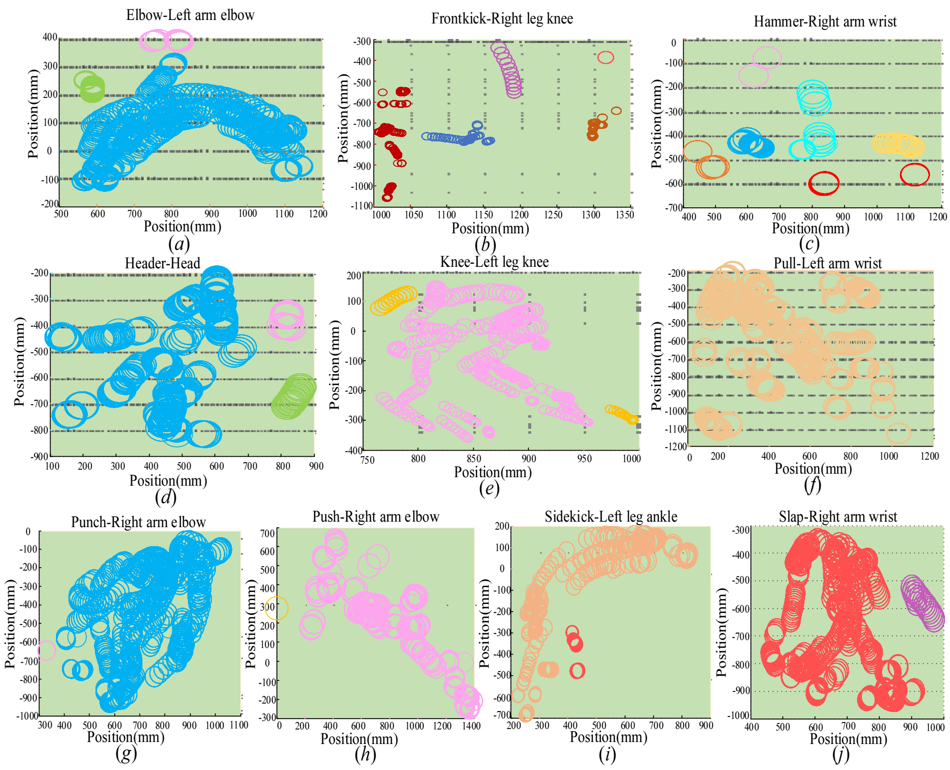

Figure 3. Trajectory of the active state

In order to construct a multi-layer of movement model of the body that is conducive to intuitively and independently expressing the shape and manner of the movement towards the human body. The head node is chosen as the root node. Left arm, right arm, left leg, right leg, inner limbs of the four limbs is treated as a category, because the changes of these nodes can be expressed a substantial move. We connect the dots of the circle of Figure 3, and they all constitute the undirected graph of the path.

In Figure 3 and Figure 4, there are two types of trajectory: linear motion and curvilinear motion. Among them, the direction of linear motion is constant and the direction of movement in the curve is constantly changing. The amplitude of the figure changes greatly, indicating that the movement speed of the limbs is fast. The reason in this change is that the movement direction of the body parts is the same as that of the external force, and the limb position is located on the same side of the direction of link movement, and the speed of the movement is fast. The change of the amplitude of the figure is small, indicating that the movement speed of the limbs is slow. The reason for this change is that the movement direction of the body part is the same as that of the external force. The part of the body is located on the opposite side of the moving direction of the link, and the speed of the movement is slow. When there is no change in the amplitude of the graph, we do not need to consider the speed of the active part of the body.

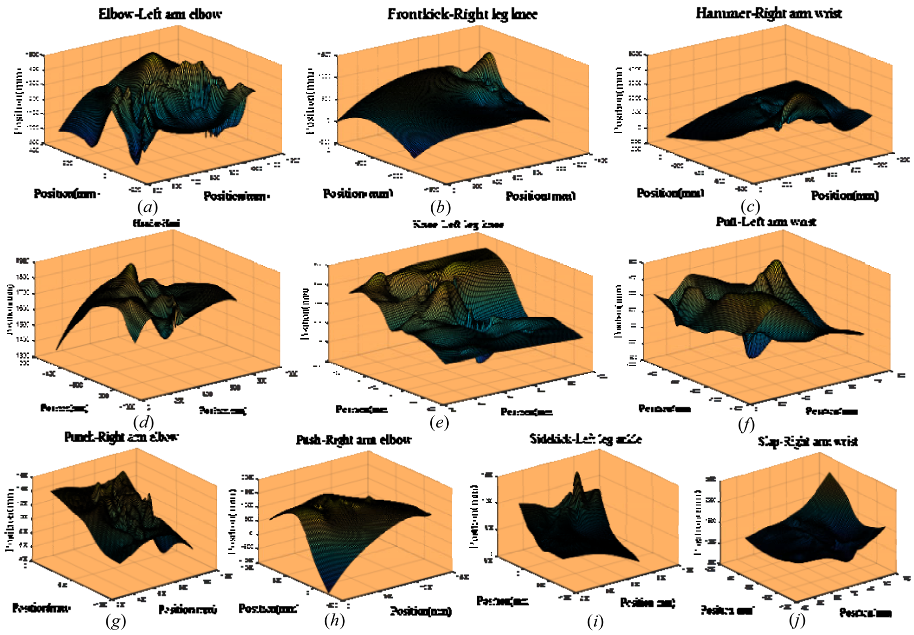

Figure 4. Three-dimensional View of the Dynamic Model of Displacement in the Active State

Based on the sample size and limb trajectory, we can predict whether the human body's motion is normal or active. Next, we collect to the active state and the normal state, ten people in nine parts of the 10 different body movements to construct the characteristic curve. Excessive behavior in the motion sequence is detected by the jump of the amplitude of the curve of motion characteristic, so as to segment the motion sequence.

As can be observed in Figure 4, most of the peaks at the graph are concentrated on one point, which is the optimal solution. The main point of the dynamic model in Figure 4 is that the height and center position of each motion is constantly changing, and the extreme point and the extreme position of each action are constantly changing. There are many dots of the local maximum in elbow, knee, pull, and punch, and many positions of the limiting are (0, 0), indicating that some places have a maximum value near (0, 0). There are many local maxima in header, but its extreme position is not (0, 0). Through the three-dimensional view of the position coordinates of the key parts of movements' body and its trajectory graph, we can know the movement characteristics of the human body. The rotation of the elbow and the upper and lower rotation of the wrist belongs to the movement of the upper limb of the human body. The elbow joint performs flexion and extension, and the trajectory of the wrist joint shows an arc shape. The shape of the ankle joint is similar to that of the ellipse, and the arc of the wrist is shaped like an arc. The main joint of the lower extremity has the ankle joint and the knee joint. The knee joint is mainly in the sagittal plane to complete the movement towards flexion, and the anklebones are mainly made of dorsal flexor and extension flexion movement in the sagittal plane.

Figure 4(a) describes the three-dimensional motion trajectories of limb movements and the three-dimensional motion graph of the body movements is described by them. Marker trajectory can represent the movement occurred during the various parts of the body's movement pattern. Elbow and left arm of the elbow makes a large range of motion and a fast frequency. The displacement of each marker point is relatively far away. The movement of the limb is rapidly rising or falling, but the rate of rise or fall is uniform. In Figure 4(b), the motion amplitude of front kicks and right leg knee is nearly stationary and the displacement between each marker point is relatively close. In Figure 4(c), the motion amplitude of hammer and right arm of the wrist is nearly stationary and the displacement between each marker point is relatively close. In Figure 4(d), the motion range of header and head is large. The frequency is fast, and the displacement between each marker point is relatively far.

Figure 4(e) shows the movement of the knee and left leg knee is large. The frequency is fast and the displacement between each marker point is relatively far away. The movement of the limb is rapidly rising or falling, but it is uniform. Figure 4(f) shows the pull and left arm has a large range of motion and a fast frequency, and the displacement between the points is relatively far away. In Figure 4(g), punch and right arm of the elbow are large, the frequency is fast, and the displacement between the points are relatively far away. In Figure 4(h), the motion amplitude of push and right arm of the wrist is nearly stationary and the displacement between each marker point is relatively close. The movement track of limbs rises or falls rapidly, and the speed of rising or falling is even. Figure 4(i) shows that the motion amplitude of the sidekick and left leg ankle is nearly stationary and the displacement between each marker point is relatively close. The movement of the limb is rapidly rising or falling, rising or falling even. Figure 4(j) shows that the motion amplitude of slap and right arm of the wrist is nearly stationary and the displacement between each marker point is relatively close.

Figure 5(a) shows that bow and head have great span, indicating that the limb motion disorder is disordered and fluctuates greatly. Its horizontal position fluctuates in the range of -15~50mm, and the ordinate position fluctuates in the range of 100~800mm. Figure 5(b) shows that the fluctuations of clap and left arm of the elbow are concentrated on two locations, its horizontal position fluctuation range is 50~170mm and 230~300mm, and the fluctuation range of the ordinate position is 550 ~ 650mm and 730 ~ 800mm. Figure 5(c) is shown that the fluctuation of handshake and left arm of the wrist is concentration, and they distribute among three places. Figure 5(d) shows that the fluctuation of hugging and right arm of the elbow is concentration, and they distribute among two places. Figure 5(e) shows that the distribution of jump and left arm of the knee is concentrated. Figure 5(f) shows that the fluctuation of the run and left leg ankle is large. Figure 5-(g) shows that seat and right leg ankle have the large span. Its horizontal position fluctuation is in the range of 55~67mm, and the ordinate position fluctuates in the range of 320~331mm. Figure 5(h) shows that the fluctuation of the stand and left leg ankle is the concentration. Figure 5(i) shows that the distribution of walk and right leg knee is sparse. Figure 5(j) shows that wave and right arm of the wrist have a slight fluctuation and a straight line movement.

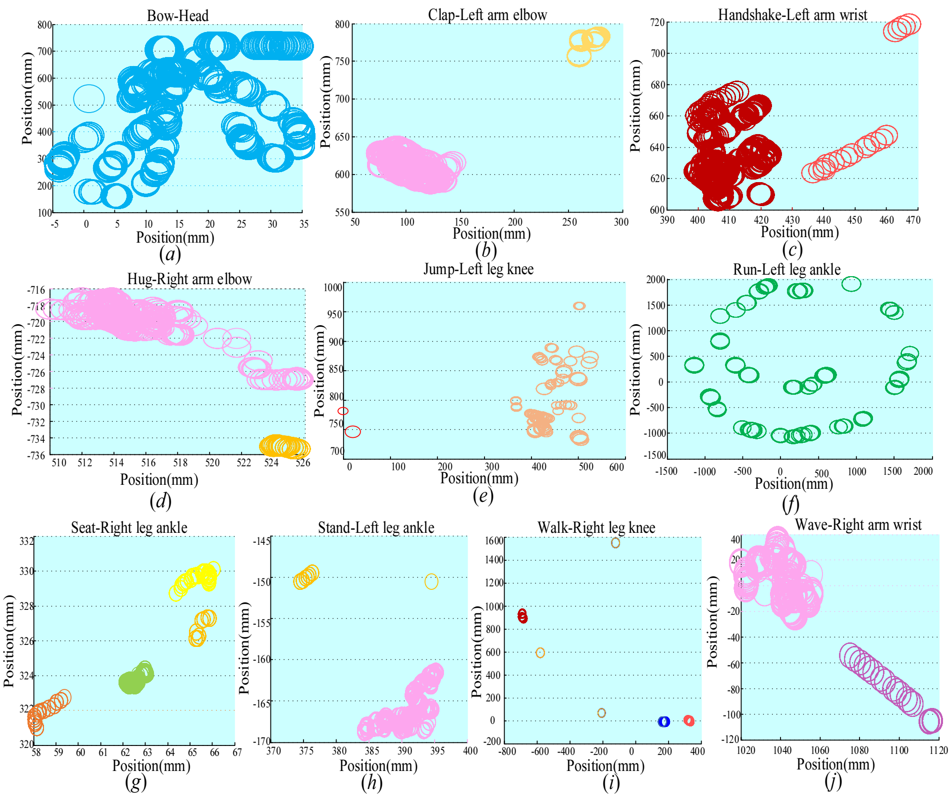

Figure 5. Change of the Movement Track of Limb Parts in Normal State

Figure 6(a) shows the movement towards the body of the bow and head is slowly rising and the increase is even. Figure 6(b) shows that the motion amplitude of clap and left arm of the elbow is nearly stationary and the displacement between each marked point is relatively close. Figure 6(c) shows the movement towards a handshake and left arm of the wrist is large, the frequency is fast, and the displacement between the points is relatively far away.

Figure 6(d) shows that the motion amplitude of hugging and right arm of the elbow is nearly stationary and the displacement between each marker point is relatively close. The trajectory of limb movement rises or falls rapidly, and the speed of ascent or descent is even. Figure 6(e) shows the motion amplitude of the jump and left arm of the knee is nearly stationary and the displacement between each marker point is relatively close. The trajectory of limb movement rises or falls rapidly, and the speed of ascent or descent is even. Figure 6(f) shows that the movement of the run and left leg ankle is relatively large, the frequency is fast and the displacement of each marker point is relatively far away. Figure 6(g) shows the motion amplitude of seat and right leg ankle is large, the frequency is fast, and the displacement between the points is relatively far away. The trajectory of limb movement rises or falls rapidly, and the speed of ascent or descent is even. Figure 6(h) shows that the motion amplitude of standing and left leg ankle is nearly stationary and the displacement between each marker point is relatively close. The trajectory of limb movement rises or falls rapidly, and the speed of ascent or descent is even. Figure 6(i) shows the motion amplitude of walk and right leg knee is large, the frequency is fast, and the displacement between the points is relatively far away. Figure 6(j) shows that the motion amplitude of wave and right arm of the wrist is nearly stationary and the displacement between each marker point is relatively close.

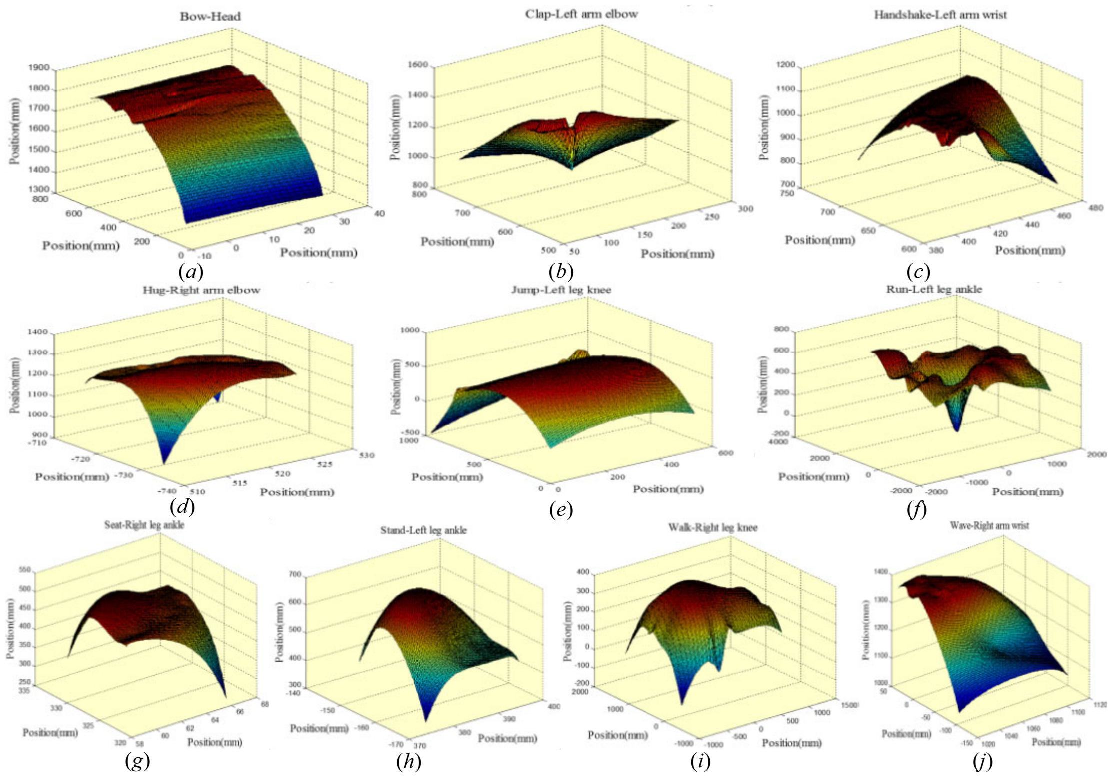

Figure 6. The position relation of different limb movements in normal state

Since there is data redundancy between VICON capturing the data onto human movement, this increases the amount of computation below. Therefore, we first adopt distributed measurement to select and pre-process the data, and the representative data represent the movement sequence. Secondly, we focus on feature extraction and recognition matching algorithm of the data on body movement.

4.2 Data Selection and Pretreatment

In the known of the data, in the body movement, the row with the missing value is first excluded. Secondly, in accordance with the standard deviation, the standard deviation of each column is obtained. The larger the standard deviation is, the more dispersed the data are. The smaller the standard deviation is, the more concentrated the data distribution is. In this way, only the column with the smallest standard deviation is reserved for the limb movements towards different positions in the same location. As a result, the redundant column data is removed, and the column data corresponding to different positions are retained as the representative (see Table 2). In order to explore the law of movement towards the human body onto the normal state and active state or complete some actions, we draw the line chart of matching the data under the normal state and the active state according to Table 2 (see Figure 7 and Figure 8). From this, we can tentatively predict what states and what parts with the body are moving for the unknown of data.

Table 2. Standard deviation in the active and normal state

Action	N	Aggressive Variables (Standard Deviation)								
Elbow	2099	V_3(25.53)	V_6(106.24)	V_9(106.97)	V_{10}(91.32)	V_{13}(119.37)	V_{18}(12.70)	V_{21}(9.26)	V_{24}(12.57)	V_{27}(8.67)
Frontkick	1778	V_3(24.13)	V_6(55.03)	V_9(79.01)	V_{12}(50.08)	V_{15}(69.31)	V_{16}(94.36)	V_{19}(88.63)	V_{22}(103.22)	V_{27}(152.09)
Hammer	1529	V_1(112.94)	V_4(184.17)	V_8(142.98)	V_{11}(177.88)	V_{14}(192.99)	V_{18}(16.59)	V_{21}(19.33)	V_{24}(17.59)	V_{27}(18.17)
Header	1208	V_3(61.32)	V_4(140.74)	V_7(190.00)	V_{10}(137.44)	V_{14}(217.27)	V_{18}(54.87)	V_{21}(104.34)	V_{24}(13.88)	V_{27}(13.91)
Knee	1208	V_3(61.32)	V_4(140.74)	V_7(190.00)	V_{12}(89.66)	V_{13}(171.03)	V_{16}(115.16)	V_{19}(140.13)	V_{22}(133.79)	V_{25}(146.69)
Pull	1664	V_3(79.09)	V_6(97.02)	V_9(120.50)	V_{12}(82.67)	V_{15}(129.22)	V_{18}(27.77)	V_{21}(46.72)	V_{24}(29.55)	V_{27}(30.25)
Punch	2206	V_3(54.06)	V_6(88.57)	V_9(150.46)	V_{12}(67.29)	V_{15}(114.86)	V_{18}(12.16)	V_{21}(15.23)	V_{24}(15.43)	V_{27}(14.06)
Push	1549	V_3(48.24)	V_6(133.42)	V_7(224.32)	V_{11}(317.51)	V_{14}(251.38)	V_{18}(33.56)	V_{21}(39.74)	V_{24}(17.17)	V_{27}(18.60)
Sidekick	1284	V_3(23.56)	V_6(86.16)	V_9(140.66)	V_{12}(75.77)	V_{15}(124.61)	V_{16}(176.48)	V_{19}(153.19)	V_{22}(74.41)	V_{25}(131.83)
Slap	1898	V_3(12.82)	V_6(73.98)	V_9(140.42)	V_{12}(87.59)	V_{15}(157.74)	V_{18}(5.86)	V_{21}(6.09)	V_{24}(8.11)	V_{27}(9.80)
Action	N	Normal Variables (Standard Deviation)								
Bow	1714	V_1(9.80)	V_4(17.67)	V_7(33.54)	V_{10}(15.67)	V_{13}(21.90)	V_{16}(2.02)	V_{19}(1.14)	V_{22}(3.66)	V_{27}(1.34)
Clap	1523	V_3(4.62)	V_4(17.31)	V_7(52.46)	V_{10}(26.56)	V_{14}(36.31)	V_{18}(0.29)	V_{21}(0.36)	V_{24}(0.23)	V_{27}(0.40)
Handshake	2273	V_1(48.86)	V_4(10.15)	V_7(13.61)	V_{11}(13.65)	V_{14}(11.43)	V_{18}(1.73)	V_{21}(0.77)	V_{24}(2.09)	V_{27}(0.88)
Hug	1752	V_3(0.74)	V_4(1.65)	V_8(3.36)	V_{10}(1.38)	V_{13}(3.23)	V_{18}(0.13)	V_{21}(0.13)	V_{24}(0.44)	V_{27}(0.19)
Jump	919	V_1(53.20)	V_4(66.21)	V_7(49.10)	V_{10}(53.93)	V_{14}(43.16)	V_{16}(53.28)	V_{21}(81.28)	V_{22}(60.26)	V_{25}(79.55)
Run	1351	V_3(39.75)	V_6(70.19)	V_9(102.76)	V_{12}(53.26)	V_{15}(90.53)	V_{18}(35.42)	V_{21}(67.55)	V_{24}(42.32)	V_{27}(764.71)
Seat	2018	V_3(0.76)	V_4(0.77)	V_7(0.45)	V_{10}(1.71)	V_{13}(1.06)	V_{18}(0.08)	V_{21}(0.96)	V_{24}(0.75)	V_{25}(0.44)
Stand	1864	V_3(1.60)	V_6(4.52)	V_8(4.21)	V_{12}(2.07)	V_{15}(1.86)	V_{18}(0.69)	V_{21}(0.64)	V_{24}(0.30)	V_{26}(0.49)
Walk	1236	V_3(11.22)	V_6(24.46)	V_9(36.98)	V_{12}(19.67)	V_{15}(29.45)	V_{18}(17.93)	V_{21}(42.07)	V_{24}(18.20)	V_{27}(34.27)
Wave	880	V_3(1.76)	V_6(5.44)	V_9(6.72)	V_{10}(26.79)	V_{13}(31.81)	V_{18}(0.83)	V_{20}(0.25)	V_{24}(0.53)	V_{26}(0.28)

The descriptive statistics of the data onto two states are analyzed, and the standard deviation of each movement towards different states are obtained. By comparing the standard deviation between the active state and the normal state, it can be observed that there is the significant difference. This indicates the accuracy and necessity of establishing the model. When the body is doing the action, the center of gravity of the body and the center of gravity of some parts of the body or the movement towards one point of the body moving in the body, forming the trajectory of each part of the body movements. Thus, displacement curves of the limb movements under active state with time are obtained, as showed Figure 7.

As can be seen from its trajectory, Figure 7(a) shows the elbow of the left arm at the wrist, left arm of the elbow, right arm of the wrist, right arm of the elbow. Figure 7(b) shows the frontkick of the left leg at the ankle, the left leg at the knee, the right leg at the knee. Figure 7(c) shows the hammer of the right leg of the angle, the left leg of the knee, the left arm of the wrist, the left arm of the elbow, the right arm of the wrist, the right arm of the elbow. Figure 7(d) shows the header of the right arm at the wrist, the left arm at the elbow, the right arm at the elbow. Figure 7(e) shows 9 limb parts in knee. Figure 7(f) shows the pull of head, the left arm of the wrist, the left arm of the elbow, the right arm of the elbow, the right arm of the wrist, the left leg of the knee and the right leg of the knee. Figure 7(g) shows the punch of the left arm at the wrist, the left arm at the elbow, the right arm at the wrist, the right arm at the elbow. Figure 7(h) shows the push of the left arm at the wrist, the left arm at the elbow, the right arm at the wrist, the right arm at the elbow. Figure 7(i) shows that except for the other eight sites of the head of the sidekick. Figure 7(j) shows the slap of the left arm at the wrist, the left arm at the elbow, the right arm at the wrist, the right arm at the elbow has the large movement, and they exhibit frequent fluctuations. The greater the extent of limb movements is, the faster the frequency is. The displacement change of other parts of the elbow, frontkick, hammer, header, pull, punch, push, the sidekick of head and slap changes in the law of fluctuations. In to slap, the displacement of the left leg of the angle, left leg knee, right leg of the angle, right leg knee close to a horizontal line, it indicates that these parts of the body are doing horizontal rectilinear motion.

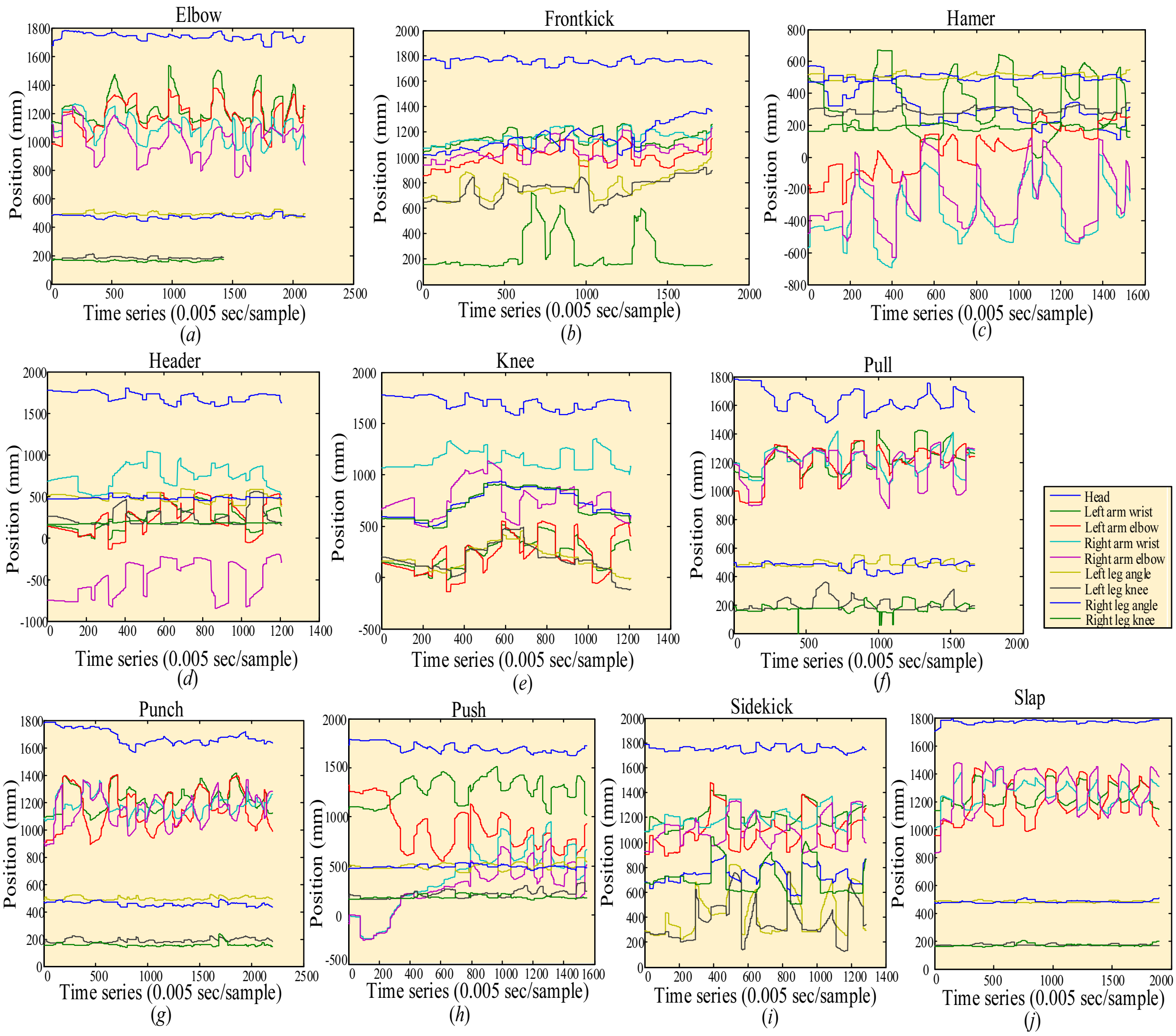

Figure 7. Distribution of limb movements in active state

Figure 7 shows that the active state of elbow, frontkick, hammers, headers, knees, pulls, punches, pushes, sidekicks and slaps represent the action trajectory of head, left arm, right arm, left leg, right leg. It includes the rule of the variation on the standard deviation trajectory, displacement and frequency of the movements of the limbs in the active state. Limb movements are expressed in images, so as to describe the process of the movement towards 10 movements towards the active state. In view of this, we can preliminaries predict the movement cycle of various body movements towards different parts in the active state. Therefore, according to the existing information and our physical characteristics of the movement of the human body, we predict that it is a movement and its next action of the corresponding point in what position.

As can be seen from its trajectory, Figure 8(a) shows the bow of the left arm at the elbow, left arm of the wrist, right arm of the wrist, right arm of the elbow. Figure 8(c) shows the handshake of the left arm at the elbow, right arm of the wrist, right arm of the elbow, right leg of the angle. Figure 8(e) shows the nine parts of the movement towards the body of jumping. Figure 8(f) shows the nine parts of the movement towards the body of running. Figure 8(i) shows the walk of the right leg at the knee, right leg of the angle, they have the large movement. The greater the extent of limb movements is, the faster the frequency is. Figure 8(a) shows the bow of the head. Figure 8(b) shows the clap of the right arm at the elbow, left arm of the elbow, right leg at the knee, right arm of the wrist. Figure 8(c) shows the handshake of the left arm at the wrist. Figure 8(i) shows the rest of the walk. Figure 8(j) shows the wave of the left arm of the wrist, left arm of the elbow, right arm of the wrist, right arm of the elbow, the motion amplitude of their parts is small, and the curves of the limbs are slowly decreasing or rising. There is no obvious fluctuation in their displacement laws, which show that the movement towards the human limb is little affected by the bow, clap, handshake, walk and wave to the normal state.

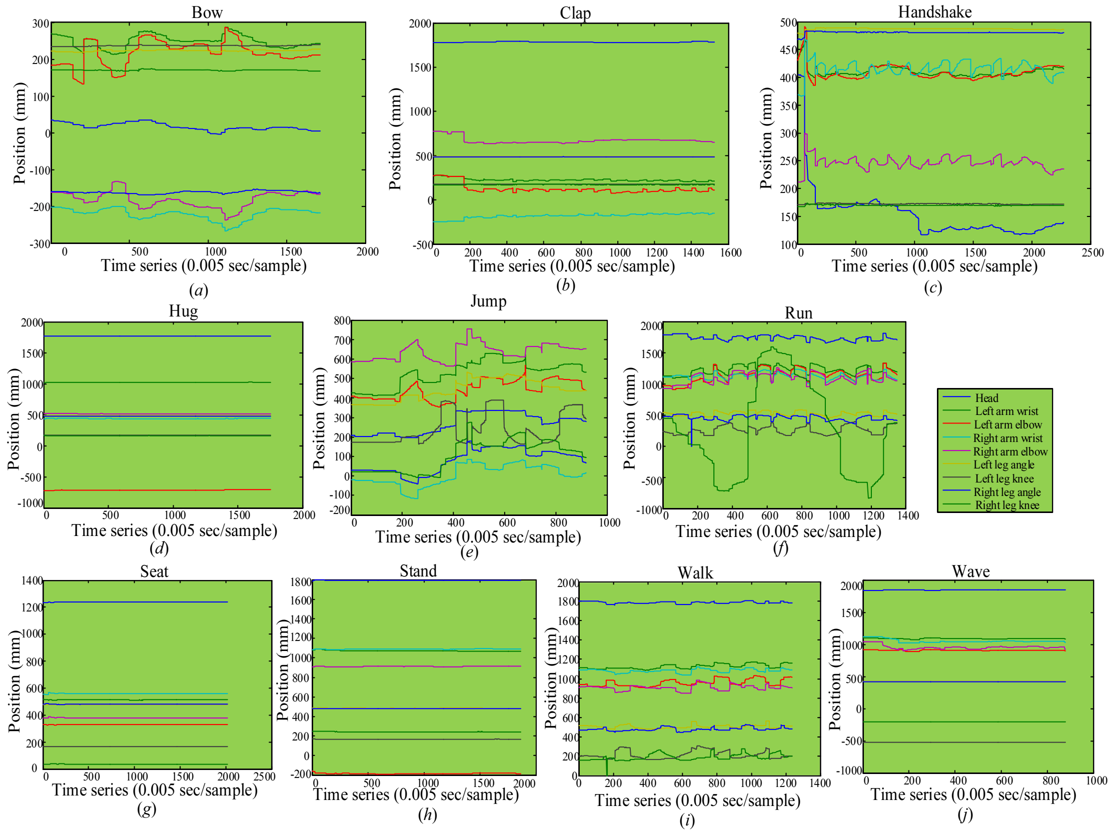

Figure 8. Distribution of limb movements in normal state

4.3 Regressions Analysis

The model of regression analysis mainly reveals the quantitative relationship between variables related to things. The quality of the extracted motion has a direct impact on the recognition of limb movements. Due to the differences between human body movements, different parts of body movements towards different body movements and different models of the body movement with different states are established through regression analysis. In order to make the results of the research to identify the movements towards the limbs, the features of the principal motions are extracted by the principal component analysis. Based on the statistical data onto the samples, regression analysis of the sample data onto body movement is made from the qualitative perspective, so as to compare the difference between the parts of the limbs in the active state and the normal state. We get the model estimation equations of the 10 actions in the active state.

Prob (F-statistic) is the significance of P value, because of P = 0.000 (approximate value), its regression equation is very significant. It is asserted that the independent variable has a significant influence on the dependent variable. The P value of the F-statistic is less than the significant level (0.05), indicating that the overall effect of the regression model is significant. And the independent variable has a significant effect on the dependent variable. At this point, the independent variable can be used to establish the regression equation. In the output of Table 3, the P values of the V_{14}, V_{24} and constant items of the header are 0.584, 0.513 and 0.356 respectively. P values of V_9 and V_{21} of punch are 0.248 and 0.286 respectively.

Elbow x_1= (-0.016, 0.058, 0.093, 0.011, 1.382, -0.304, 0.257, -0.373) (V_6, V_9, V_{10}, V_{13}, V_{18}, V_{21}, V_{24}, V_{27})'+895.213

Frontkick x_2= (0.738, -0.425, 0.763, -0.506, -0.023, 0.138, -0.098, -0.033) (V_6, V_9, V_{12}, V_{15}, V_{16}, V_{19}, V_{22}, V_{27})'+1023.635

Hammer x_3= (-0.083, -0.209, -0.223, -0.137, 5.467, -4.711, -12.758, 10.474) (V_4, V_8, V_{11}, V_{14}, V_{18}, V_{21}, V_{24}, V_{27})'+3219.965

Header x_4= (-0.797, 0.455, 0.047, 1.449, -0.372, 1.453) (V_4, V_7, V_{10}, V_{18}, V_{21}, V_{27})'

Knee x_5= (-0.130, 0.095, 0.048, 0.033, -0.135, 0.274, -0.038, -0.058) (V_4, V_7, V_{12}, V_{13}, V_{16}, V_{19}, V_{22}, V_{25})'+1680.640

Pull x_6= (-0.135, -0.108, -0.319, 0.542, -0.690, 1.377, -0.953) (V_6, V_9, V_{12}, V_{18}, V_{21}, V_{24}, V_{27})'+1755.827

Punch x_7= (-0.154, -0.156, 0.121, -0.276, 2.652, -0.805) (V_6, V_{12}, V_{15}, V_{17}, V_{24}, V_{27})'+708.116

Push x_8= (-0.025, 0.076, -0.234, 0.162, 0.071, 0.320, 0.186, 0.094) (V_6, V_7, V_{11}, V_{14}, V_{18}, V_{21}, V_{24}, V_{27})'+1499.825

Sidekick x_9= (0.566, -0.388, 0.342, -0.199, -0.103, 0.099, 0.032, -0.064) (V_6, V_9, V_{12}, V_{15}, V_{16}, V_{19}, V_{22}, V_{25})'+1327.660

Slap x_{10}= (0.084, -0.014, 0.093, 0.019, 0.496, -0.251, 2.202, -1.447) (V_6, V_9, V_{12}, V_{15}, V_{18}, V_{21}, V_{24}, V_{27})'+530.837

Table 3. Model estimation of 10 actions in aggressive state

Elbow	Coefficient	Prob.	Frontkick	Coefficient	Prob.	Hammer	Coefficient	Prob.	Header	Coefficient	Prob.
V_6	-0.016	0.004	V_6	0.738	0.000	V_4	-0.083	0.000	V_4	-0.797	0.000
V_9	0.058	0.000	V_9	-0.425	0.000	V_8	-0.209	0.000	V_7	0.455	0.000
V_{10}	0.093	0.000	V_{12}	0.763	0.000	V_{11}	-0.223	0.000	V_{10}	0.047	0.000
V_{13}	0.011	0.033	V_{15}	-0.506	0.000	V_{14}	-0.137	0.000	V_{14}	-0.003	0.584
V_{18}	1.382	0.000	V_{16}	-0.023	0.014	V_{18}	5.467	0.000	V_{18}	1.449	0.000
V_{21}	-0.304	0.000	V_{19}	0.138	0.000	V_{21}	-4.711	0.000	V_{21}	-0.372	0.000
V_{24}	0.257	0.000	V_{22}	-0.098	0.000	V_{24}	-12.758	0.000	V_{24}	-2.895	0.513
V_{27}	-0.373	0.000	V_{27}	-0.033	0.000	V_{27}	10.474	0.000	V_{27}	1.453	0.000
C	895.213	0.000	C	1023.635	0.000	C	3219.965	0.000	C	2251.163	0.356
Knee	Coefficient	Prob.	Pull	Coefficient	Prob.	Punch	Coefficient	Prob.	Push	Coefficient	Prob.
V_4	-0.130	0.000	V_6	-0.135	0.000	V_6	-0.154	0.000	V_6	-0.025	0.000
V_7	0.095	0.000	V_9	-0.108	0.000	V_9	0.014	0.248	V_7	0.076	0.000
V_{12}	0.048	0.000	V_{12}	-0.319	0.000	V_{12}	-0.156	0.000	V_{11}	-0.234	0.000
V_{13}	0.033	0.000	V_{15}	-0.039	0.047	V_{15}	0.121	0.000	V_{14}	0.162	0.000
V_{16}	-0.135	0.000	V_{18}	0.542	0.000	V_{17}	-0.276	0.000	V_{18}	0.071	0.034
V_{19}	0.274	0.000	V_{21}	-0.690	0.000	V_{21}	-0.049	0.286	V_{21}	0.320	0.000
V_{22}	-0.038	0.011	V_{24}	1.377	0.000	V_{24}	2.652	0.000	V_{24}	0.186	0.000
V_{25}	-0.058	0.000	V_{27}	-0.953	0.000	V_{27}	-0.805	0.000	V_{27}	0.094	0.000
C	1680.640	0.000	C	1755.827	0.000	C	708.116	0.00	C	1499.825	0.000
Sidekick	Coefficient	Prob.	Slap	Coefficient	Prob.						
V_6	0.566	0.000	V_6	0.084	0.000						
V_9	-0.388	0.000	V_9	-0.014	0.019						
V_{12}	0.342	0.000	V_{12}	0.093	0.000						
V_{15}	-0.199	0.000	V_{15}	0.019	0.000						
V_{16}	-0.103	0.000	V_{18}	0.496	0.000						
V_{19}	0.099	0.000	V_{21}	-0.251	0.000						
V_{22}	0.032	0.031	V_{24}	2.202	0.000						
V_{25}	-0.064	0.000	V_{27}	-1.447	0.000						
C	1327.660	0.000	C	530.837	0.000						

According to Table 1 and the above of the regression equation, there is a significant negative correlation: Elbow and left arm(ELB), right arm(WRS), right leg(ANK). Frontkick and right arm(ELB), right leg(KNE), left arm(WRS), left leg(ANK), right leg(ANK). Hammer and left arm(ELB), right arm(ELB), left leg(KNE), right leg(KNE), right arm(WRS), left leg(ANK). Header and right arm(ELB), left leg(KNE), left arm(WRS), right leg(ANK). Knee and left arm(ELB), left arm(WRS), left leg(ANK), right leg(ANK). Pull and left arm(ELB), right arm(ELB), left leg(KNE), right arm(WRS), right leg(ANK). Punch and left arm(ELB), left leg(KNE), left arm(WRS), right leg(ANK). Push and left arm(ELB), left leg(KNE). Sidekick and right arm(ELB), right leg(KNE), left arm(WRS), right leg(ANK). Slap and right arm(ELB), right arm(WRS), right leg(ANK). There is a significant positive correlation: Elbow and right arm(ELB), left leg(KNE), right leg(KNE), left arm(WRS), left leg(ANK). Frontkick and left arm(ELB), left leg(KNE), right arm(WRS). Hammer and left arm(WRS), right leg(ANK). Header and left arm(ELB), right arm(WRS). Knee and right arm(ELB), left leg(KNE), right leg(KNE), right arm(WRS). Pull and left arm(WRS), left leg(ANK). Punch and right Leg(KNE), left leg(ANK). Push and right arm(ELB), right leg(KNE), left arm(WRS), right arm(WRS), left leg(ANK), right leg(ANK). Sidekick and left arm(ELB), left leg(KNE), right arm(WRS), left leg(ANK). Slap and left arm(ELB), left leg(KNE), right leg(KNE), left arm(WRS), left leg(ANK). In normal state, the model of 10 actions is estimated.

As can be seen from Table 4, the P value of V_{19} of the bow is 0.060, the P value of V_{22} of the jump is 0.967, the P value of V_{24} and V_{27} of the run are 1.000 and 0.425 respectively, the P value of V_{24} of the walk is 0.109, the P value of V_{18} of the wave is 0.808, t which is eliminated.

Bow y_1= (0.438, -0.228, 0.099, -0.050, 0.990, -0.109, 0.129) (V_4, V_7, V_{10}, V_{13}, V_{16}, V_{22}, V_{27})'-152.182

Clap y_2= (-0.339, 0.163, 0.023, -0.153, 6.339, -4.164, 0.897, -0.841) (V_4, V_7, V_{10}, V_{14}, V_{18}, V_{21}, V_{24}, V_{27})' -728.661

Handshake y_3= (7.067, -3.899, -2.697, 3.048, -11.282, 14.812, -2.696, 2.501) (V_4, V_7, V_{11}, V_{14}, V_{18}, V_{21}, V_{24}, V_{27})'+3031.541

Hug y_4= (-0.074, -0.036, 0.095, 0.175, 0.516, 0.412, -0.147, 0.662) (V_4, V_8, V_{10}, V_{13}, V_{18}, V_{21}, V_{24}, V_{27})'+1320.259

Jump y_5= (0.484, -0.106, 0.509, -0.033, -0.015, 0.026, 0.042) (V_4, V_7, V_{10}, V_{14}, V_{16}, V_{21}, V_{25})'+76.663

Run y_6= (0.472, -0.329, 0.839, -0.266, 0.016, -0.008) (V_6, V_9, V_{12}, V_{15}, V_{18}, V_{21})'+871.928

Table 4. Model estimation of 10 kinds of actions in normal state

Bow	Coefficient	Prob.	Clap	Coefficient	Prob.	Handshake	Coeffieicnt	Prob.	Hug	Coefficient	Prob.
V_4	0.438	0.000	V_4	-0.339	0.000	V_4	7.067	0.000	V_4	-0.074	0.000
V_7	-0.228	0.000	V_7	0.163	0.000	V_7	-3.899	0.000	V_8	-0.036	0.000
V_{10}	0.099	0.000	V_{10}	0.023	0.000	V_{11}	-2.697	0.000	V_{10}	0.095	0.000
V_{13}	-0.050	0.027	V_{14}	-0.153	0.000	V_{14}	3.048	0.000	V_{13}	0.175	0.000
V_{16}	0.990	0.000	V_{18}	6.339	0.000	V_{18}	-11.282	0.000	V_{18}	0.516	0.000
V_{19}	-0.584	0.060	V_{21}	-4.164	0.000	V_{21}	14.812	0.000	V_{21}	0.412	0.000
V_{22}	-0.109	0.000	V_{24}	0.897	0.002	V_{24}	-2.696	0.000	V_{24}	-0.147	0.000
V_{27}	0.129	0.000	V_{27}	-0.841	0.001	V_{27}	2.501	0.000	V_{27}	0.662	0.000
C	-152.182	0.002	C	-728.661	0.003	C	3031.541	0.000	C	1320.259	0.000
Jump	Coefficient	Prob.	Run	Coefficient	Prob.	*Seat*	Coefficient	Prob.	Stand	Coefficient	Prob.
V_4	0.484	0.000	V_6	0.472	0.000	V_4	-0.064	0.035	V_6	0.216	0.000
V_7	-0.106	0.000	V_9	-0.329	0.000	V_7	0.176	0.000	V_8	-0.059	0.000
V_{10}	0.509	0.000	V_{12}	0.839	0.000	V_{10}	0.567	0.000	V_{12}	-0.161	0.000
V_{14}	-0.033	0.001	V_{15}	-0.266	0.000	V_{13}	-0.880	0.000	V_{15}	0.115	0.000
V_{16}	-0.015	0.000	V_{18}	0.016	0.000	V_{18}	-0.349	0.000	V_{18}	-0.049	0.014
V_{21}	0.026	0.000	V_{21}	-0.008	0.027	V_{21}	-0.159	0.016	V_{21}	-0.348	0.000
V_{22}	0.0003	0.967	V_{24}	1.35E-06	1.000	V_{24}	-0.574	0.000	V_{24}	1.700	0.000
V_{25}	0.042	0.000	V_{27}	-0.003	0.425	V_{25}	-0.960	0.000	V_{26}	0.549	0.000
C	76.663	0.000	C	871.928	0.000	C	1733.133	0.000	C	748.087	0.000
Walk	Coefficient	Prob.	Wave	Coefficient	Prob.						
V_6	0.237	0.000	V_6	-0.293	0.000						
V_9	-0.260	0.000	V_9	0.078	0.000						
V_{12}	1.084	0.000	V_{10}	0.038	0.000						
V_{15}	-0.474	0.000	V_{13}	-0.036	0.000						
V_{18}	-0.004	0.000	V_{18}	0.008	0.808						
V_{21}	0.022	0.000	V_{20}	-1.567	0.000						
V_{24}	0.002	0.109	V_{24}	1.402	0.000						
V_{27}	-0.019	0.000	V_{26}	0.297	0.020						
C	1017.875	0.000	C	740.793	0.000						

Seat y_7= (-0.064, 0.176, 0.567, -0.880, -0.349, -0.159, -0.574, -0.960) (V_4, V_7, V_{10}, V_{13}, V_{18}, V_{21}, V_{24}, V_{25})'+1733.133

Stand y_8= (0.216, -0.059, -0.161, 0.115, -0.049, -0.348, 1.700, 0.549) (V_6, V_8, V_{12}, V_{15}, V_{18}, V_{21}, V_{24}, V_{26})'+748.08

Walk y_9= (0.237, -0.260, 1.084, -0.474, -0.004, 0.022, -0.019) (V_6, V_9, V_{12}, V_{15}, V_{18}, V_{21}, V_{27})'+1017.875

Wave y_{10}= (-0.293, 0.078, 0.038, -0.036, -1.567, 1.402, 0.297) (V_6, V_9, V_{10}, V_{13}, V_{20}, V_{24}, V_{26})'+740.793

We cannot determine the activity and normal body movements based on the information obtained. In this case, depending on Table 2, the standard deviation is smaller, and the action is stable. Then the better simulation result is chosen as the theoretical model. In the active state, we select V_{27} in elbow, V_3 in frontkick, V_{18} in the hammer, V_{27} in the header, V_3 in the knee, V_{18} in the pull, V_{27} in punch, V_{24} in a push, V_{18} in a sidekick, V_3 in slap. In the normal state, we select V_{19} in the bow, V_{24} in the clap, V_{21} in the handshake, V_{18} in the hug, V_{14} in jump, V_3 in run, V_{18} in seat, V_{24} in stand, V_{26} in walk, V_3 in waves. Therefore, we establish the model estimation equations in the active and normal state according to Eviews.

In the probable value of the significant level of the F statistic: the P values of frontkick(x_2) and knee(x_5) are 0.334 and 0.110 respectively in the active state. In the normal state, the P values of the handshake(y_3), stand(y_8) and walk(y_9) are 0.918, 0.162 and 0.049, respectively, and then be eliminated.

Active state X= (0.057, -0.137, 0.018, 0.140, -0.080, 0.054, 0.204) (x_3, x_4, x_6, x_7, x_8, x_9, x_{10})'-47.915

Normal state Y= (2.435, 0.734, 0.007, -0.016, -4.779, -2.098) (y_2, y_4, y_5, y_6, y_7, y_{10})'+741.537

In the active state, when the action of hammering(x_3) increases by one unit, the action of X increases by 0.057. When the action of the header(x_4) increases by one unit, the action of X reduces by 0.137. When the action of pulling(x_6) increases by one unit, the action of X increases by 0.018. When the action of the punch(x_7) increases by one unit, the action of X increases by 0.140. When the action of pushing(x_8) increases by one unit, the action of X reduces by 0.080. When action of sidekick(x_9) increases by one unit, the action of X increases by 0.054. When the action of slap(x_{10}) increases by one unit, the action of X increases by 0.204. In the normal state, when the action of clap (y_2) increases by one unit, the action of Y increases by 2.435. When the action of hug (y_4) increases by one unit, the action of Y increases by 0.734. When the action of jumping (y_5) increases by one unit, the action of Y increases by 0.007. When the action of running (y_6) increases by one unit, the action of Y reduces by 0.016. When action of seat (y_7) increases by one unit, the action of Y reduces by 4.779. When the action of the wave (y_{10}) increases by one unit, the action of Y reduces by 2.098.

5 Conclusions

In order to solve the problem of the recognition of body movement, ten kinds of movement experiments are studied in nine parts of 10 individuals in normal and active states. Furthermore, change of displacement of time series in action is taken as the characteristic model of body movement. The feature vectors are extracted by regression analysis, and the feature vectors are extracted to represent an action class. An action class is represented by a feature vector, which reduces the complexity of the data and improves the efficiency. Different people indicate different movement towards characters of various states. They show different characteristics of movement. Therefore, depending on a given data, matching the model to identify body motion accurately is our goal of researching. Through the human body movement data, we applied the method of the body movement using function recognition. It can be applied to animation production and game development, making animation more close to the real action of human beings, and improving the visual effect of animation. At the same time, the method can also be applied to the difficult effects of movies, which greatly promote the technological development of the film industry. The recognition of body movement is realized through the trajectory of human motion and the equation of movement.

Acknowledgements

This work is supported by National Natural Science Foundation of China (Grant No. 11561017, 61972160, 61662019, 61701487 and 61601262). Natural Science Foundation of Hainan Province (No. 117212). Innovation Foundation of Chinese Academy of Sciences (Grant No. CXJJ-17-M126).

References

[1] C. P. Townsend, S W. Arms, *Posture and Body Movement Measuring System*, US6834436, December, 2004.

[2] G. Castellano, S. D. Villalba, A. Camurri, Recognising Human Emotions from Body Movement and Gesture Dynamics, *International Conference on Affective Computing and Intelligent Interaction*, Berlin, Heidelberg, 2007, pp. 71-82.

[3] C. Richter, K. Moran, B. Marshall, N. E. O'Connor, Identification of Movement Strategies in Vertical Jumps, *32 International Conference of Biomechanics in Sports*, Johnson City, TN, USA, 2014, pp. 340-343.

[4] X. Yang, *Human Motion Pattern Recognition Based on a Single Acceleration Sensor*, South China University of Technology Press, 2011.

[5] Q. Huang, *A Human-machine Interaction Technology Based on Gyroscope Sensors*, Xiangtan University Press, 2011.

[6] H. Lau, K. Tong, The Reliability of Using Accelerometer and Gyroscope for Gait Event Identification on Persons with Dropped Foot, *Gait & Posture*, Vol. 27, No. 2, pp. 248-257, February, 2008.

[7] A. K. Bourke, G. M. Lyons, A Threshold-based Fall-detection Algorithm Using a Bi-axial Gyroscope Sensor, *Medical Engineering & Physics*, Vol. 30, No. 1, pp. 84-90, January, 2008.

[8] O. Amft, H. Junker, G. Troster, Detection of Eating and Drinking Arm Gestures Using Inertial Body-worn Sensors, *Proceedings 9th IEEE International Symposium on Wearable Computers,* Osaka, Japan, 2005, pp.160-163.

[9] J. Pansiot, B. Lo, G. Z. Yang, Swimming Stroke Kinematic Analysis with BSN, *International Conference on Body Sensor Network*s, Singapore, 2010, pp. 153-158.

[10] D. K. Arvind, A. Valtazanos, Speckled Tango Dancers: Real-Time Motion Capture of Two-Body Interactions Using On-body Wireless Sensor Networks, *International Workshop on Wearable and Implantable Body Sensor Networks*, Berkeley, CA, USA, 2009, pp. 312-317.

[11] H. Liu, *Research on Human Body Reorientation Technology Based on Motion Constraints*, Yanshan University Press, 2013.

[12] P. Kejonen, K. Kauranen, H. Vanharanta, Body Movements in Postural Balance with Motion Analysis, *European Journal of Physical and Rehabilitation Medicine*, 1998.

[13] H. Chen, M. Xue, Z. Mei, S. B. Oetomo, W. Chen, A Review of Wearable Sensor Systems for Monitoring Body Movements of Neonates, *Sensors*, Vol. 16, No. 12, pp. 2134, December, 2016.

[14] A. Islam, Md. Asikuzzaman, M. A. Garratt, M. R. Pickering, 3D Kinematic Measurement of Human Movement Using Low Cost Fish-eye Cameras, *Eighth International Conference on Graphic and Image Processing*, Tokyo, Japan, 2016, pp. 29-31.

[15] S. K. Saripalle, G. C. Paiva, R. R. Derakhshani, G. W. King, C. T. Lovelace, Classification of Body Movements Based on Posturographic Data, *Human Movement Science*, Vol. 33, No. 1, pp. 238-250, February, 2014.

[16] M. Sadeghi, M. E. Andani, F. Bahrami, M. Parnianpour. Trajectory of Human Movement during Sit to Stand: A New Modeling Approach Based on Movement Decomposition and Multi-phase Cost Function, *Experimental Brain Research*, Vol. 229, No. 2, pp. 221-234, September, 2013.

[17] K. Yashiro, M. Fujii, O. Hidaka, K. Takada, Kinematic Modeling of Jaw-closing Movement during Food Breakage, *Journal of Dental Research*, Vol. 80, No. 11, pp. 20-30, November, 2015.

[18] J A. Kleman, *Three Dimensional Body Movement Structure*, US20180036584, 2018.

[19] S. Caudron, H. Ceyte, P.-A. Barraud, C. Cian, M. Guerraz, Perception of Body Movement When Real and Simulated

Displacements Are Combined, *Plos One*, Vol.13, No. 3, pp. 193-194, March, 2018.

[20] G. Orgs, A. Dovern, N. Hagura, P. Haggard, G. R. Fink, P. H. Weiss, Constructing Visual Perception of Body Movement with the Motor Cortex. *Cerebral Cortex*, Vol. 26, No. 1, pp. 440-449, January, 2016.

[21] T. T. Simpson, S. L. Wiesner, B. C. Bennett, Dance Recognition System Using Lower Body Movement, *Journal of Applied Biomechanics*, Vol. 30, No. 1, pp. 147-153, February, 2014.

Biographies

Biyuan Yao is currently pursuing her Ph.D. degree in School of Computer Science and Engineering, South China University of Technology, Guangzhou, China. Her research interests include applications of image processing and pattern recognition, communication and graph theory with applications.

Jianhua Yin is Professor of Hainan University, MS supervisor. His research interests include graph theory with applications.

Guiqing Li currently works at the School of Computer Science and Engineering, South China University of Technology, Guangzhou, China. His research interests focus on fields related to Computer Graphics such as digital geometry processing, dynamic geometry processing, and image and video processing.

Hui Zhou received B.S. degree from University of Science and Technology of China (USTC), and Ph.D. degree from University of Chinese Academy of Science. Dr. Zhou has worked in IBM China Research Laboratory for several years, and has been an associate professor of Hainan University since 2011. Dr. Zhou is in charge of several research projects including the National Natural Science Funds projects. His research interests include writing robot, data visualization, cluster file system.

Lixin Liu received the B.S. degree, M.S. degree and Ph.D. degree from the Harbin Engineering University, P. R. China, in 2008, 2011, and 2015, respectively. He is working as an assistant professor in the Institute of Deep-sea Science and Engineering, Chinese Academy of Sciences. His research interests include image processing, communication and deep learning. He is a member of the IEEE.